

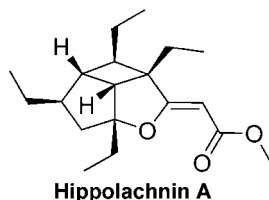
# Hippolachnin A, a New Antifungal Polyketide from the South China Sea Sponge *Hippospongia lachne*

Shu-Juan Piao,<sup>†,||</sup> Yun-Long Song,<sup>‡,||</sup> Wei-Hua Jiao,<sup>†,||</sup> Fan Yang,<sup>§</sup> Xiang-Fang Liu,<sup>†</sup> Wan-Sheng Chen,<sup>†</sup> Bing-Nan Han,<sup>\*,§</sup> and Hou-Wen Lin<sup>\*,†,§</sup>

Laboratory of Marine Drugs, Department of Pharmacy, Changzheng Hospital, Second Military Medical University, Shanghai 200003, P. R. China, Department of Medicinal Chemistry, School of Pharmacy, Second Military Medical University, Shanghai 200433, P. R. China, and Department of Pharmacy, Renji Hospital, Affiliated to School of Medicine, Shanghai Jiaotong University, Shanghai 200127, P. R. China  
franklin67@126.com; bingnanh@hotmail.com

Received April 25, 2013; Revised Manuscript Received June 28, 2013

## ABSTRACT



Hippolachnin A

Hippolachnin A (**1**), a polyketide possessing an unprecedented carbon skeleton with a four-membered ring, was isolated from the South China Sea sponge *Hippospongia lachne*. The structure was elucidated using MS and NMR spectroscopic analyses, and the absolute configuration was determined using a calculated ECD method. Hippolachnin A demonstrated potent antifungal activity against three pathogenic fungi, *Cryptococcus neoformans*, *Trichophyton rubrum*, and *Microsporum gypseum*, with a MIC value of 0.41  $\mu$ M for each fungus.

For many years, diverse marine organisms have inspired researchers to identify novel marine natural products with pharmaceutical potential.<sup>1</sup> Marine sponges (Porifera) are one of the richest sources of bioactive secondary metabolites with chemical diversity. Sponges of the genus *Hippospongia* are well recognized as a rich source of terpenoids, such as sesquiterpenes,<sup>2</sup> sesterterpenes,<sup>3</sup> furanoterpenes,<sup>4</sup>

triterpenoic acids,<sup>5</sup> and fatty acid derivatives.<sup>6</sup> These compounds exhibit antitumor,<sup>7</sup> anti-inflammatory,<sup>8</sup> and antifungal<sup>9</sup> activity. As part of our continuing efforts to discover bioactive marine natural products from South China Sea sponges,<sup>10</sup> bioassay-guided isolation of a portion of the EtOH extract of *H. lachne* with antifungal activity, collected off the Xisha Islands, resulted in the purification of an unprecedented polyketide, hippolachnin A (**1**), and

<sup>†</sup> Changzheng Hospital, Second Military Medical University.

<sup>‡</sup> School of Pharmacy, Second Military Medical University.

<sup>§</sup> Renji Hospital, Shanghai Jiaotong University.

<sup>||</sup> These authors contributed equally.

(1) Mayer, A. M. S.; Glaser, K. B.; Cuevas, C.; Jacobs, R. S.; Kem, W.; Little, R. D.; McIntosh, J. M.; Newman, D. J.; Potts, B. C.; Shuster, D. E. *Trends Pharmacol. Sci.* **2010**, *31*, 255–265.

(2) (a) Ishibashi, M.; Ohizumi, Y.; Cheng, J. F.; Nakamura, H.; Hirata, Y.; Sasaki, T.; Kobayashi, J. *J. Org. Chem.* **1988**, *53*, 2855–2858. (b) Kobayashi, J.; Naitoh, K.; Sasaki, T.; Shigemori, H. *J. Org. Chem.* **1992**, *57*, 5773–5776. (c) Shen, Y. C.; Chen, C. Y.; Kuo, Y. H. *J. Nat. Prod.* **2001**, *64*, 801–802.

(3) (a) Musman, M.; Ohtani, I. I.; Nagaoka, D.; Tanaka, J.; Higa, T. *J. Nat. Prod.* **2001**, *64*, 350–352. (b) Piao, S. J.; Zhang, H. J.; Lu, H. Y.; Yang, F.; Jiao, W. H.; Yi, Y. H.; Chen, W. S.; Lin, H. W. *J. Nat. Prod.* **2011**, *74*, 1248–1254.

(4) Rifai, S.; Fassouane, A.; Kijjoa, A.; Soest, R. V. *Mar. Drugs* **2004**, *2*, 147–153.

(5) Craig, K. S.; Williams, D. E.; Hollander, I.; Frommer, E.; Mallon, R.; Collins, K.; Wojciechowski, D.; Tahir, A.; Soest, R. V.; Andersen, R. J. *Tetrahedron Lett.* **2002**, *43*, 4801–4804.

(6) Ishiyama, H.; Ishibashi, M.; Ogawa, A.; Yoshida, S.; Kobayashi, J. *J. Org. Chem.* **1997**, *62*, 3831–3836.

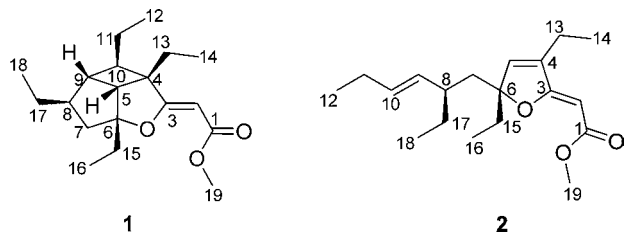
(7) Liu, H. W.; Wang, G. H.; Namikoshi, M.; Kobayashi, H.; Yao, X. S.; Cai, G. P. *Pharm. Biol.* **2006**, *44*, 522–527.

(8) Oda, T.; Wang, W. F.; Ukai, K.; Nakazawa, T.; Mochizuki, M. *Mar. Drugs* **2007**, *5*, 151–156.

(9) Lee, H. S.; Lee, T. H.; Yang, S. H.; Shin, H. J.; Shin, J.; Oh, K. B. *Bioorg. Med. Chem. Lett.* **2007**, *17*, 2483–2486.

(10) (a) Liu, X. F.; Song, Y. L.; Zhang, H. J.; Yang, F.; Yu, H. B.; Jiao, W. H.; Piao, S. J.; Chen, W. S.; Lin, H. W. *Org. Lett.* **2011**, *13*, 3154–3157. (b) Zhang, H. J.; Yi, Y. H.; Yang, G. J.; Hu, M. Y.; Cao, G. D.; Yang, F.; Lin, H. W. *J. Nat. Prod.* **2010**, *73*, 650–655. (c) Jiao, W. H.; Huang, X. J.; Yang, J. S.; Yang, F.; Piao, S. J.; Gao, H.; Li, J.; Ye, W. C.; Yao, X. S.; Chen, W. S.; Lin, H. W. *Org. Lett.* **2012**, *1*, 202–205.

its proposed biogenic precursor,  $\alpha,\beta$ -unsaturated methyl ester (**2**),<sup>11</sup> which was recently disclosed as a PPAR $\gamma$  antagonist.<sup>11d</sup> Hippolachnin A (**1**) exhibited potent antifungal activity against three pathogenic fungi (*Cryptococcus neoformans*, *Trichophyton rubrum*, and *Microsporum gypseum*) with an MIC value of 0.41  $\mu$ M for all three species.



Hippolachnin A (**1**)<sup>12</sup> was isolated as a colorless oil. This compound's molecular formula was established as C<sub>19</sub>H<sub>30</sub>O<sub>3</sub> with five degrees of unsaturation with an HRESIMS ion peak at  $m/z$  329.2092 [M + Na]<sup>+</sup>. The IR absorption bands at 2927, 1635, and 1217 cm<sup>-1</sup> indicated the presence of an  $\alpha,\beta$ -unsaturated ester subunit. The <sup>1</sup>H NMR spectrum showed the presence of four ethyl groups through four triplet methyl groups at  $\delta_H$  0.88 (6H, t,  $J$  = 7.5 Hz, 2  $\times$  CH<sub>3</sub> overlapped), 1.02 (3H, t,  $J$  = 7.5 Hz), and 0.80 (3H, t,  $J$  = 7.5 Hz), a methoxy signal at  $\delta_H$  3.66 (3H, s), and an olefinic proton at  $\delta_H$  4.56 (s) (Table 1). The <sup>13</sup>C and DEPT NMR spectra displayed 19 carbons, including four quaternary carbons (an ester carbonyl carbon at  $\delta_C$  167.3, an oxygenated sp<sup>2</sup> carbon at  $\delta_C$  181.1, an oxygenated sp<sup>3</sup> carbon at  $\delta_C$  104.2, and an aliphatic carbon at  $\delta_C$  56.6); five methine groups at  $\delta_C$  83.5, 49.4, 47.5, 46.3, and 52.9; five methylene peaks at  $\delta_C$  45.1, 30.8, 28.3, 24.6, and 23.3; and five methyl groups at  $\delta_C$  8.6, 9.6, 11.8, 13.0, and 50.4 (Table 1). The above-mentioned data indicated that **1** possessed one double bond and one carbonyl group, which accounted for two out of the five degrees of unsaturation, implying the presence of three rings in the structure.

The structure of **1** was further established after interpreting 2D NMR experiments (Figure 1). The <sup>1</sup>H–<sup>1</sup>H COSY correlations of H<sub>2</sub>-13/H<sub>3</sub>-14, H<sub>2</sub>-11/H<sub>3</sub>-12, H<sub>2</sub>-15/H<sub>3</sub>-16, and H<sub>2</sub>-17/H<sub>3</sub>-18 indicated the presence of four ethyl groups, meanwhile the correlations of H-5/H-9, H-8/H-7b, and H<sub>2</sub>-17/H-8 revealed the linkage of CH-5/CH-9 and CH<sub>3</sub>-18/CH<sub>2</sub>-17/CH-8/CH<sub>2</sub>-7, respectively (Figure 1). Accordingly, the connectivity of the above subunits with the remaining atoms enabled assembly into the planar structure of **1** by interpreting the HMBC spectrum in detail. HMBC correlations from both H<sub>3</sub>-14 and H<sub>2</sub>-13 to C-4, and H<sub>2</sub>-13 to C-3, C-5, and C-10 placed the ethyl CH<sub>2</sub>-13/CH<sub>3</sub>-14 on C-4 as well as linked three carbon bonds, C-3/C-4, C-4/C-10, and C-4/C-5. This assignment

was confirmed by HMBC correlations of H-5/C-10, C-13 and H-10/C-4, C-13. Due to the overlap of H-10/H-15a, and H-9/H-13a in the <sup>1</sup>H NMR spectrum, the HMBC cross peaks of H-9 with C-4, C-11, and C-10 could not be clearly distinguished. Fortunately, the HMBC correlations from H-8 to C-10, from H<sub>2</sub>-17 to C-7, C-8, and C-9, and from both H-10 and H<sub>2</sub>-11 to C-9 could be clearly observed, which not only placed the ethyl CH<sub>2</sub>-17/CH<sub>3</sub>-18 at C-8 and linked the carbon bond C-8/C-9 but also revealed the presence of a cyclobutane moiety.

Furthermore, H<sub>2</sub>-15 showed HMBC correlations with C-5, C-6, and C-7, which connected a cyclopentane moiety and located the ethyl CH<sub>2</sub>-15/CH<sub>3</sub>-16 at C-6. The remaining ethyl was placed at C-10 on account of the long-ranged correlations of H-11b with C-4, C-9, and C-10. Consequently, a 4/5-fused bicyclic system was unambiguously established.

Moreover, a pair of <sup>4</sup> $J$  correlations from both H-15a and H-15b to C-3 was observed in the HMBC spectrum (Figure 1 and Figure S11 in Supporting Information (SI)), which indicated the presence of an ether between C-3 and C-6 and formed a tetrahydrofuran ring, accounting for their downfield chemical shifts of C-6 and C-3 and the remaining one degree of unsaturation.

In addition, HMBC correlations from the olefinic proton H-2 to C-1, C-3, and C-4 and from the methoxy H<sub>3</sub>-19 to C-1 suggested the  $\alpha,\beta$ -unsaturated ester was located at C-4, which was confirmed by the <sup>3</sup> $J$  correlation between H<sub>2</sub>-13 and C-3. Thus, the planar structure of **1** was finally determined as shown in Figure 1.

The geometry of double bond  $\Delta^{2,3}$  was determined as *Z* based on the NOESY correlation between H-2 and H-13b and was confirmed by comparison of the chemical shift of proton H-2 ( $\delta_H$  4.56) with data in the literature ( $\delta$  4.85 for *Z*,  $\delta$  5.23 for *E*).<sup>13</sup>

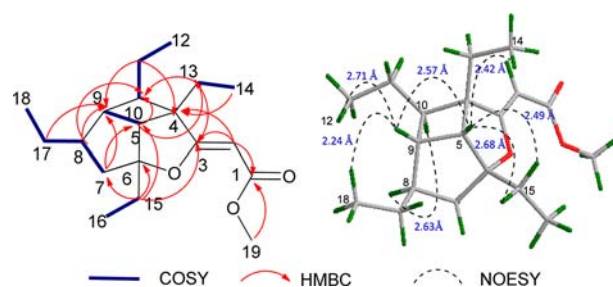


**Figure 1.** Key COSY, HMBC, and NOESY correlations of **1**.

The relative configuration of **1** was determined using a NOESY spectrum (Figure 1). The observed key NOESY correlations of H-5 with H-9, H<sub>3</sub>-14, and H<sub>2</sub>-15, as well as H-9 with H<sub>3</sub>-12 and H<sub>3</sub>-18, implicated the *cis* orientation of H-9/H-5 and their relative *sin* relationships with the other ethyl groups on the 4,5-fused rings (Figure 1;

(11) (a) Stierle, D.; Faulkner, D. *J. Org. Chem.* **1980**, *45*, 3396–3401. (b) Schmidt, E.; Faulker, D. *Tetrahedron Lett.* **1996**, *37*, 6681–6684. (c) Yanai, M.; Ohta, S.; Ohta, E.; Hirata, T.; Ikegami, S. *Bioorg. Med. Chem.* **2003**, *11*, 1715–1721. (d) Festa, C.; Lauro, G.; De Marino, S.; D'Auria, M. V.; Monti, M. C.; Casapullo, A.; D'Amore, C.; Renga, B.; Mencarelli, A.; Petek, S.; Bifulco, G.; Fiorucci, S.; Zampella, A. *J. Med. Chem.* **2012**, *55*, 8303–8317.

(12) Hippolachnin A (**1**), colorless oil; [ $\alpha$ ]<sub>D</sub><sup>23</sup> +27° (*c* 0.12, MeOH); UV (MeOH)  $\lambda_{max}$  (log  $\epsilon$ ) 253 (4.11) nm; IR (KBr)  $\nu_{max}$  3435, 2927, 1635, 1458, 1375, 1217, 1039, 802 cm<sup>-1</sup>; <sup>1</sup>H and <sup>13</sup>C NMR data, see Table 1; HRESIMS  $m/z$  329.2092 [M + Na]<sup>+</sup> (calcd for C<sub>19</sub>H<sub>30</sub>O<sub>3</sub>Na, 329.2093).

(13) Ueoka, R.; Nakao, Y.; Kawatsu, S.; Yaegashi, J.; Matsumoto, Y.; Matsunaga, S.; Furihata, K.; Van Soest, R. W. M.; Fusetani, N. *J. Org. Chem.* **2009**, *74*, 4204–4207.

Figures S15, S16). The NOESY correlation of H-8/H-10 (Figure S17) suggested a *sin* relationship between these two protons oriented to the geometry of 4,5-fused rings. As a result, we proposed a *trans* configuration of H-9 and H-10 on the cyclobutane, owing to the severe unfavorable distortions of the sp<sup>3</sup> atoms involved in the interested rings for the alternative anti-arrangement of the above protons.

**Table 1.** <sup>1</sup>H NMR (500 MHz) and <sup>13</sup>C NMR (125 MHz) Data of **1** in CDCl<sub>3</sub>

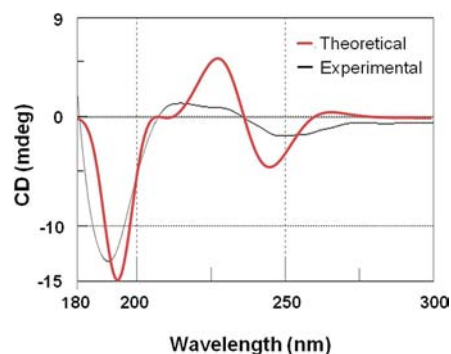
no.	δ <sub>H</sub> , (J in Hz)	δ <sub>C</sub>	HMBC	NOESY
1		167.3		
2	4.56, s	83.5	1, 3, 4	H-13a, H <sub>3</sub> -14
3		181.1		
4		56.6		
5	2.59, d, 8.0	49.4	3, 4, 6, 7, 8, 9, 10, 13, 15	H-9, 15a, H <sub>3</sub> -14
6		104.2		
7a	2.44, q, 7.5	45.1	6, 13, 15	
7b	1.32, m		17	
8	1.98, m	47.5	9, 10	H-10, 17a, 18
9	1.79, m	46.3	4, 10, 11	H-11, H <sub>3</sub> -12, 18
10	1.82, m	52.9	5, 8, 9	H-8
11a	1.64, m	24.6	9, 10	H-9, 11b
11b	1.32, m		4, 9, 10	H-11a
12	0.88, 3H, t, 7.5	11.8	4, 10, 11	H-11a, 11b
13a	1.75, m	23.3	3, 5	H-5, H <sub>3</sub> -14
13b	1.52, m		3, 5, 10	H-2, H <sub>3</sub> -14
14	0.80, 3H, t, 7.5	8.6	4, 13	H-2, 5, 13b
15a	1.82, m	30.8	3, 5, 7, 16	H-5, 7a, 15b
15b	1.67, m		3, 6	H-15a
16	1.02, 3H, t, 7.5	9.6	6, 15	H-5, 7a, 15a
17a	1.33, m	28.3	7, 8, 9, 18	H-5, 8
17b	1.30, m		7, 8, 9	
18	0.88, 3H, t, 7.5	13.0	8, 17	H-7a, 9, 17a
19	3.66, 3H, s	50.4	1	

The calculated ECD method was used to establish the absolute configuration of **1** (Figure 2).<sup>14</sup> The stereostructure of **1** was constructed on the basis of the distance constraints from the key correlations observed in the NOESY spectrum. Using these spectroscopic data, only the stereoisomer shown in Figure 1 and its corresponding mirror image were found to satisfy the observed NOE constraints. Therefore, only two configurations were generated for theoretical calculations to identify the most probable candidate for **1**. A conformational search was then performed using Sybyl 8.03 software with a simulated annealing method and the MMFF94 force field. The 24 corresponding minimum geometries were fully optimized using DFT at the B3LYP/6-31G(d) level, as implemented in the Gaussian 03 program package. All of them displayed no imaginary frequencies. Initially, the global minimum energy-minimized structures of two probable configurations of **1** were submitted to ECD calculations using the

TDDFT method. The calculated ECD spectrum of **1** was compared with the experimental ECD spectrum to determine the most probable configuration (Figure S21). Finally, with the aid of Multiwfn 3.2 software,<sup>15</sup> the Boltzmann-averaged ECD spectrum of **1** was obtained to provide a clear comparison with the experimental data (Figure 2).

The global minimum geometry was also used for GIAO-based <sup>13</sup>C NMR chemical shift calculations to gain further supporting data for the carbon assignments of **1**.<sup>16</sup> The experimental and calculated <sup>13</sup>C NMR chemical shifts (relative to TMS-resonance calculated at the same level of DFT) were listed in Table S1 of the SI. The calculated isotropic shielding constants were in good correlation with the experimental <sup>13</sup>C NMR chemical shifts (Figure S20 in SI). After linear scaling,<sup>17</sup> the mean absolute error with respect to the experimentally observed chemical shifts was only 1.70 ppm for **1**. The largest absolute error was 3.60 ppm on C10, which might reflect the effect of the strained spirocycle system. Accordingly, the quantum-mechanical GIAO calculations of the <sup>13</sup>C NMR chemical shifts provide a reliable basis for the correct carbon assignments in **1**.

As shown in Figure 2, there was satisfactory agreement between the stimulated and experimental ECD spectrum of **1**. The computed ECD spectrum for the structure at 4*S*, 5*R*, 6*R*, 8*R*, 9*R*, 10*R* clearly reproduced both the sign and shape of the measured ECD spectrum. Thus, the absolute configuration of **1** was unambiguously established as 4*S*, 5*R*, 6*R*, 8*R*, 9*R*, 10*R*.

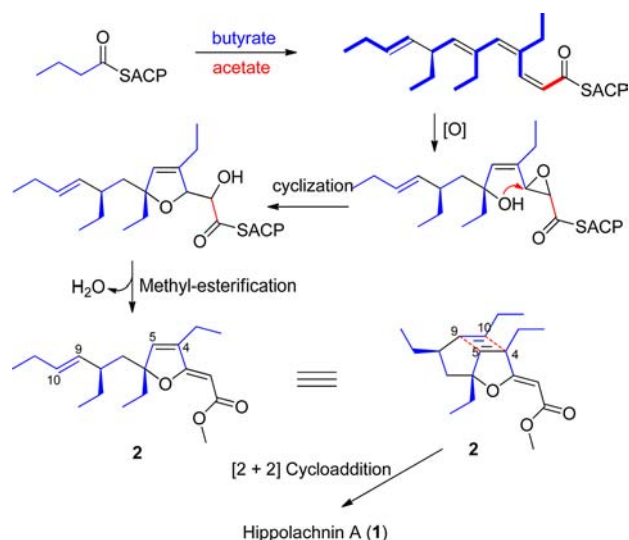


**Figure 2.** Experimental and theoretical ECD spectra for hippolachnin A (**1**).

A plausible biogenetic pathway for Hippolachnin A (**1**) is proposed in Scheme 1. The ethyl branches are hypothesized to be assembled in part from butyrate units.<sup>18</sup> Four butyrate units and an acetate unit are required to construct

(14) (a) Berova, N.; Di Bari, L.; Pescitelli, G. *Chem. Soc. Rev.* **2007**, 36, 914–931. (b) Menna, M.; Aiello, A.; D'Aniello, F.; Imperatore, C.; Luciano, P.; Vitalone, R.; Irace, C.; Santamaria, R. *Eur. J. Org. Chem.* **2013**, 3241–3246.

(15) Lu, T.; Chen, F. *J. Comput. Chem.* **2012**, 33, 580–592.  
 (16) (a) Helgaker, T.; Jaszunski, M.; Ruud, K. *Chem. Rev.* **1999**, 99, 293–352. (b) Aliev, A. E.; Courtier-Murias, D.; Zhou, S. *THEOCHEM* **2009**, 893, 1–5.  
 (17) Lodewyk, M. W.; Siebert, M. R.; Tantillo, D. J. *Chem. Rev.* **2012**, 112, 1839–62.  
 (18) (a) Huang, X.-H.; van Soest, R.; Roberge, M.; Andersen, R. J. *Org. Lett.* **2003**, 6, 75–78. (b) Kubanek, J.; Andersen, R. *Tetrahedron Lett.* **1997**, 38, 6327–6330.

**Scheme 1.** Plausible Biosynthetic Pathway of **1**

the polyketide skeleton. Following a series of oxidation, cyclization, elimination reactions and methyl-esterification at C-1, the intermediate **2** is produced. A four-membered ring was formed via an intramolecular [2 + 2] cycloaddition reaction between  $\Delta^{4,5}$  and  $\Delta^{9,10}$  of **2**. Finally, the metabolite **1** was generated via methyl-esterification at C-1.

Hippolachnin A (**1**) was evaluated for antifungal activity against seven pathogenic fungi using ketoconazole (KCZ), voriconazole (VCZ), fluconazole (FCZ), and terbinafine (TBF) as positive controls (Table 2). Hippolachnin A exhibited potent antifungal activity against *Cryptococcus neoformans*, *Trichophyton rubrum*, and *Microsporum gypseum*, with a MIC value of 0.41  $\mu$ M for all three species and moderate activity against four other fungi strains. The results showed that hippolachnin A (**1**) is a promising new lead compound for antifungal therapy. The cytotoxic activity of **1** on human cancer cell lines HCT-116, A549, and HeLa was also evaluated using the MTT method<sup>19</sup> but

(19) Carmichael, J.; De Graff, W. G.; Gazdar, A. F.; Minna, J. D.; Mitchell, J. B. *Cancer Res.* **1987**, *47*, 936–942.

**Table 2.** Antifungal activity of hippolachnin A (**1**) against seven pathogenic fungi

fungi	<b>1</b>	MIC ( $\mu$ M)			
		KCZ	VCZ	FCZ	TBF
<i>Cryptococcus neoformans</i>	0.41	0.12	0.18	3.27	13.7
<i>Candida albicans</i>	13.1	0.47	0.18	6.54	3.44
<i>Candida glabrata</i>	1.63	0.12	0.18	6.54	3.44
<i>Cryptococcus parapsilosis</i>	1.63	1.88	0.18	6.54	27.5
<i>Aspergillus fumigatus</i>	13.1	7.53	5.73	209	3.44
<i>Trichophyton rubrum</i>	0.41	0.12	0.09	1.63	0.43
<i>Microsporum gypseum</i>	0.41	0.24	0.18	0.82	0.43

showed no significant inhibitory activity on these cancer lines.

**Acknowledgment.** The authors thank Prof. Jin-He Li (Institute of Oceanology, Chinese Academy of Sciences) for identifying the marine sponge and Yong-Bing Cao for the antifungal activity evaluation (R & D Center of New Drug, School of Pharmacy, Second Military Medical University). The authors are grateful for the helpful discussions provided by Prof. Harald Gross (Department of Pharmaceutical Biology, University of Tübingen) and Prof. Jian Zhang (Shanghai Jiaotong University). This research was supported by the National Natural Science Fund for Distinguished Young Scholars of China (81225023), the National Natural Science Fund of China (Nos. 81072573, 81172978, 81001394, 41106127, and 81173635), and Shanghai Subject Chief Scientist (12XD1400200). We are also grateful for the financial support of the National High Technology Research and Development Program of China (863 Projects, Nos. 2011AA09070107 and 2013AA092902) and the Gaussian 03 computational service of Shanghai Super Computing Center. In commemoration of Prof. Xin-Sheng Yao's 80th birthday.

**Supporting Information Available.** Experimental procedures, HRESIMS, IR, 1D NMR, and 2D NMR spectra of hippolachnin A (**1**). This material is available free of charge via the Internet at <http://pubs.acs.org>.

The authors declare no competing financial interest.